

Untargeted Metabolomic Analyses Reveal Chemical Complexity of Dioecious *Cannabis* Flowers

Matthew T. Welling,^A Myrna A. Deseo,^{A,B} Antony Bacic,^{A,B} and Monika S. Doblin^{A,B,C}

^ALa Trobe Institute for Agriculture and Food, Department of Animal, Plant and Soil Sciences, School of Life Sciences, AgriBio Building, La Trobe University, Bundoora, Vic. 3086, Australia.

^BAustralian Research Council Research Hub for Medicinal Agriculture, AgriBio Building, La Trobe University, Bundoora, Vic. 3086, Australia.

^CCorresponding author. Email: m.doblin@latrobe.edu.au

Cannabis is a mostly dioecious multi-use flowering plant genus. Sexual dimorphism is an important characteristic in *Cannabis*-based commercial production systems, which has consequences for fibre, seed, and the yield of secondary metabolites, such as phytocannabinoid and terpenes for therapeutic uses. Beyond the obvious morphological differences between male and female plants, metabolic variation among dioecious flowers is largely undefined. Here, we report a pilot metabolomic study comparing staminate (male) and pistillate (female) unisexual flowers. Enrichment of the α -linolenic acid pathway and consensus evaluation of the jasmonic acid (JA) related compound 12-oxo-phytodienoic acid (OPDA) among differentially abundant metabolites suggests that oxylipin signalling is associated with secondary metabolism and sex expression in female flowers. Several putative phytocannabinoid-like compounds were observed to be upregulated in female flowers, but full identification was not possible due to the limitation of available databases. Targeted analysis of 14 phytocannabinoids using certified reference standards (cannabidiolic acid (CBDA), cannabidiol (CBD), Δ^9 -tetrahydrocannabinolic acid A (Δ^9 -THCAA), Δ^9 -tetrahydrocannabinol (Δ^9 -THC), cannabichromenic acid (CBCA), cannabichromene (CBC), cannabigerolic acid (CBGA), cannabigerol (CBG), cannabinolic acid (CBNA), cannabinol (CBN), cannabidivarinic acid (CBDVA), cannabidivarin (CBDV), tetrahydrocannabivarinic acid (THCVA), and tetrahydrocannabivarin (THCV)) showed a higher total phytocannabinoid content in female flowers compared with the male flowers, as expected. In summary, the development of a phytocannabinoid-specific accurate-mass MSⁿ fragmentation spectral library and gene pool representative metabolome has the potential to improve small molecule compound annotation and accelerate understanding of metabolic variation underlying phenotypic diversity in *Cannabis*.

Keywords: liquid chromatography, mass spectrometry, phytochemistry, metabolism, *Cannabis*, cannabinoids, untargeted metabolomics, flowering.

Received 30 January 2021, accepted 26 April 2021, published online 21 May 2021

Introduction

Cannabis, a member of the family Cannabaceae, is a highly heterozygote multi-use anemophilous (wind pollinated) flowering plant genus, which is believed to have originated in Central Asia.^[1] Taxonomic assignment and speciation of *Cannabis* is unresolved.^[2] Despite this ambiguity, a monotypic status is widely supported on the basis that physiological and genetic barriers to gene flow are underreported.^[3] Domestication of *Cannabis* over prolonged periods of time has led to its global dispersal. Fossil evidence in the form of pollen deposits and seed remains suggest widespread use across Eurasia dating back several thousand years.^[1,4] In addition to traditional uses for food and fibre, plants also have recreational and medicinal value due to their secondary metabolites, particularly phytocannabinoids and terpenes.

Cannabis plants are prolific producers of secondary metabolites, with their repertoire spanning several chemical classes

including terpenoids, flavonoids, stilbenoids, alkaloids and phenolic amides.^[5] However, it is the group of isoprenylated resorcinyl polyketides, commonly referred to as phytocannabinoids, that *Cannabis* is most recognised for on account of their exclusivity to this taxon and their recreational and potential therapeutic uses.^[6] The phytocannabinoid Δ^9 -tetrahydrocannabinol (THC), which is a partial agonist of the human endocannabinoid CB₁ receptor,^[7] is primarily responsible for the narcotic status of this plant. A large proportion of the more than 100 phytocannabinoid constituents are non-intoxicating, with a subset representing molecules of potential therapeutic importance. These include cannabidiol (CBD) which is the active ingredient in Epidiolex, a United States Food and Drug Administration (FDA) approved prescription medicine for the treatment of intractable seizures in childhood epileptic disorders.^[8] Terpenes which are also produced by *Cannabis* are thought to contribute to phytocannabinoid ligand activity, although

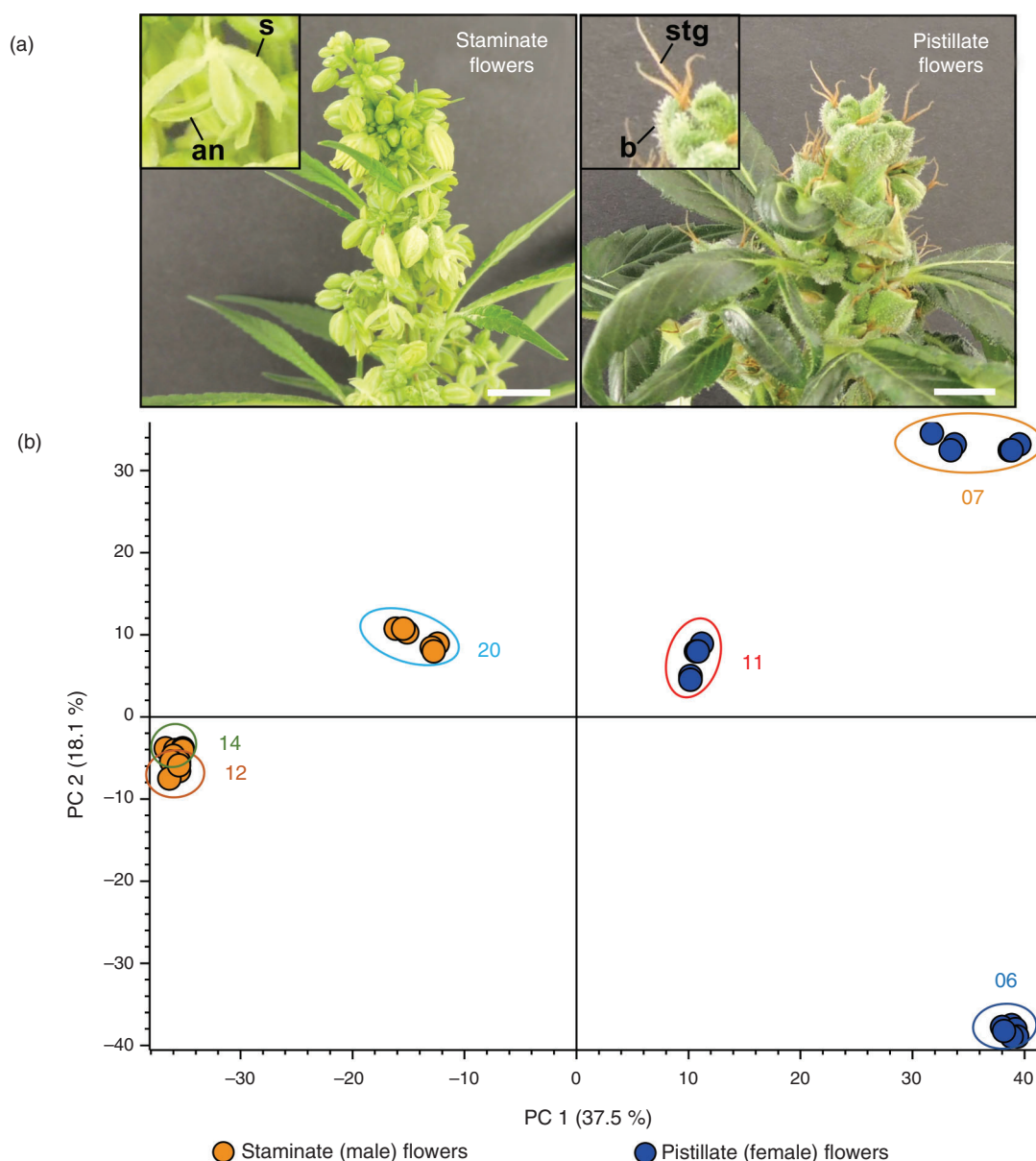


Fig. 1. Principal component analysis of metabolite abundances from male and female floral tissue samples. (a) Images of *Cannabis sativa* accession 06 staminate (male) and pistillate (female) flowers. Insert of staminate flowers shows sepal (s) and anther (an) of male flower. Insert of pistillate flower shows perigonal bract (b) and mature stigma (stg) of female flower. Scale Bar = 1 cm. (b) PCA performed on 2599 putative metabolites identified from male and female floral tissue samples identified by UHPLC-ESI-HRMS in the positive mode. Floral samples derived from six *Cannabis* accessions. Numbers overlaid on PCA plot represent accession IDs (Table 1).

evidence for the so-called ‘entourage effect’ when extended to terpenoids is largely anecdotal.^[9]

An arbitrary level of THC content, which can vary by jurisdiction, is used to demarcate crop use, with a low THC content in female flowers congruent with industrial hemp end-uses.^[10] Plants typically segregate into one of three chemotypes based on THC/CBD ratio, although this system of classification does not account for variation of other phytocannabinoid constituents such as those with altered alkyl groups which can be more abundant than either THC or CBD.^[11] The biosynthesis of phytocannabinoids and other secondary metabolites, such as terpenoids, is concentrated within specialised capitate stalked glandular trichomes.^[12] These are hair-like structures which are abundant on the epidermal surfaces of floral tissues of female

inflorescences.^[13] Unisexual female inflorescences are highly branched compound racemes that are comprised of monophotometric structures consisting of an axillary shoot, solitary pistillate flowers, subtending bracts, and reduced leaves.^[14] In contrast, male inflorescences have sparse leaf coverage and consist largely of pendulous panicles.^[15] Staminate flowers have a five-sepal enclosed androecium, which, on opening, allows for longitudinal release of pollen grains (Fig. 1a).^[15]

Being mainly dioecious, *Cannabis* segregates into distinct female and male plants, although monocious phenotypes with bisexual flowers or inflorescences bearing separate male and female flowers occur to a lesser extent.^[15,16] Reproductive commitment occurs as early as the emergence of the fourth leaflet pair.^[15] Sex expression can be influenced by temperature

and photoperiod, although not all genotypes are strictly obligate in this regard and sensitivity to photoperiodic induction can vary considerably amongst germplasm.^[17] Sex is determined by heteromorphic X and Y chromosomes.^[18] Males are the heterogametic sex (XY) while females are the homogametic (XX) sex.^[18] However, sexual phenotype can be modified in well differentiated male as well as female plants by various chemical and phytohormonal applications, such as silver thiosulfate, gibberellic acid, and ethephon.^[19–21]

Sexual dimorphism is a critical factor in *Cannabis*-based production systems and is essential for genetic improvement of germplasm.^[22] For phytocannabinoid production, genetically female plants are grown in the absence of pollen. Male and hermaphroditic plants have less floral biomass, reduced phytocannabinoid yield, and also negatively impact female inflorescence quality via fertilisation and initiation of seed development.^[16] Prolonged virginity in female plants during flowering also aids in the formation of congested pistillate inflorescences which improves phytocannabinoid yield.^[16,23] Conversely, monoecy can be desirable for the cultivation of industrial hemp. Not only does this reduce crop heterogeneity, but also mitigates early flowering and senescence of unisexual male plants which can complicate mechanical harvesting of both stems and seed. However, the monoecious state can be inter-generationally unstable and sexual phenotypic extremes can vary from predominantly male to predominantly female.^[24]

Despite the commercial importance of sexual dimorphism in *Cannabis*, few studies have comprehensively examined chemical phenotypes of male and female flowers. While comparisons have been made between unisexual flowers, these have either been targeted towards a small number of phytocannabinoids or have been applied to a narrow subset of the gene pool.^[25–28] Ultra-high-performance liquid chromatography–electrospray ionisation–high-resolution mass spectrometry (UHPLC-ESI-HRMS) with data-dependent acquisition is an effective analytical technique for untargeted chemical profiling of plant constituents, as it facilitates chromatographic separation of complex matrices and simultaneous acquisition of HRMS and MSⁿ spectral data.^[29] Here, we performed a pilot study comparing the floral tissues of three male and three female industrial hemp accessions to establish the veracity of the methodological approach and the minimal sampling requirements for a large-scale germplasm comparison of *Cannabis* chemotypes. Both a targeted approach with consideration of 14 phytocannabinoid constituents as well as a non-targeted approach using UHPLC-ESI-HRMS methodology was performed with the aim of bridging the gap in understanding the metabolic variation underlying sexual phenotype in *Cannabis*.

Results

Metabolic Variation Among *Cannabis* Flowers

A panel of six industrial hemp accessions were grown from seed in a controlled environment room. As is common practice for indoor-grown *Cannabis*, seedlings were grown initially under a long-day photoperiod to promote vegetative growth and then under a short-day photoperiod to initiate flowering. The time it took plants to reach flower maturity varied among accessions. Female plants used for analysis were harvested ~4 (accession 11) and ~5 (accessions 06 and 07) weeks after exposure to a short-day photoperiod when ~95 % of the stigma on pistillate (hereafter referred to as female) flowers were browned and shrivelled, while male plant individuals were harvested after a period of ~5 (accession 20) and ~7 weeks (accession 12 and 14) following photoperiod induction when ~95 % staminate (hereafter referred to as male) flowers had opened and expelled pollen (Table 1). No consistent differences in height were observed between male and female plants within sample groups, with female and male plants varying from 1.4 m (accessions 06 and 12) to ~2 m (accessions 07 and 14). To enrich for sex-specific flowers and capture within-plant metabolic variation, foliage leaves, seeds, and/or stems were removed from inflorescences before analysis and floral tissues were sampled from the apical and basal inflorescence of each male and female plant.

Untargeted metabolic analysis was performed using UHPLC-ESI-HRMS and data-dependent MS² acquisition. Preliminary method development involving *Cannabis* floral tissues showed an increase in the number of features and coverage of the metabolome in positive ion mode as compared with negative ion mode (data not shown) and so untargeted analysis and quantification of unknown compounds was performed in positive ion mode. The representative total ion chromatogram (TIC) from the six accessions showed a high level of dissimilarity (Fig. 2), indicating that the floral samples had diverse chemical profiles. Analysis of male and female floral tissues across all accessions generated 74 151 features that accounted for 5161 putative compounds distinguishable by retention time and molecular weight. The compound list was filtered by eliminating those that fall within the group with low abundant chromatographic peak areas < 50 000 and those lacking MS² fragmentation spectra. After filtering, 2599 compounds/metabolites remained in the list (Supplementary Material, Table S1). Principal component analysis (PCA) of the 2599 putative metabolites showed a clear separation of male and female flower samples, with the first two principal components (PCs) accounting for 37.5 % (PC1) and 18.1 % (PC2) of the variability in the dataset (Fig. 1b and Supplementary Material, Fig. S1). Processing of putative

Table 1. Genetic materials used for targeted and untargeted metabolomic analysis

Accession ID	Accession	Taxon	Subtaxon	Sex	Source
06	2019_S_0006	<i>Cannabis sativa</i> L.	Industrial hemp	Female	Southern Cross University ^A
07	2019_S_0007	<i>Cannabis sativa</i> L.	Industrial hemp	Female	The Hemp Corporation Pty Ltd ^B
11	2019_S_0011	<i>Cannabis sativa</i> L.	Industrial hemp	Female	Midlands Seed Pty Ltd ^C
12	2019_S_0012	<i>Cannabis sativa</i> L.	Industrial hemp	Male	The Hemp Corporation Pty Ltd ^B
14	2019_S_0014	<i>Cannabis sativa</i> L.	Industrial hemp	Male	The Hemp Corporation Pty Ltd ^B
20	2019_S_0020	<i>Cannabis sativa</i> L.	Industrial hemp	Male	The Hemp Corporation Pty Ltd ^B

^ASouthern Cross University, Military Rd, East Lismore, NSW 2480, Australia.

^BThe Hemp Corporation Pty Ltd, 513 Fishers Hill Road, Vacy, NSW 2421, Australia.

^CMidlands Seed Pty Ltd, 323 Prossers Road, Richmond, Tas. 7025, Australia.

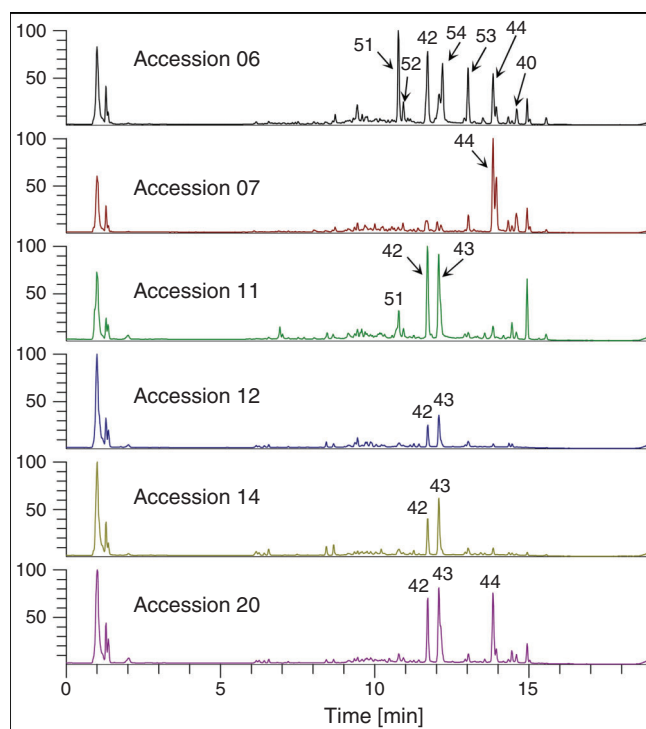


Fig. 2. Total ion chromatogram (TIC) of methanol extracts of *Cannabis* floral tissues from different accessions. Major peaks are labelled with compound identification of known cannabinoids based on comparison of MS data and retention time with certified reference standards: Δ^9 -THCAA (40); CBDA (42); CBD (43); Δ^9 -THC (44); CBDVA (51); CBDV (52); THCA (53); and THC (54).

metabolites by hierarchical clustering analysis (HCA) grouped technical (extraction) replicates by accession and by inflorescence position (apical and basal; descending developmental maturity) as well as by male and female flowers. Floral samples from the six accessions formed two major clades representative of male and female flowers, suggesting that unisexual flowers have distinct metabolomes (Fig. 3a).

Analysis of Differentially Abundant Metabolites (DAMs) of Cannabis Floral Tissues

Analysis of DAMs between male and female floral samples indicated a greater number of metabolites were upregulated in the female floral tissues as compared with the male (Fig. 3b). Of the 2599 putative metabolites, 861 were upregulated while 626 were downregulated in female versus male flowers (P -value of < 0.05 , \log_2 fold change ≥ 1.5) (Fig. 3b). A large proportion of putative metabolite abundances ($\sim 43\%$) were shared between male and female flowers (shaded in grey in Fig. 3b). Metabolites common to both unisexual flowers were dismissed and only DAMs were investigated further.

To gain an overall understanding of metabolic variation between female and male floral samples, and to interpret the biological significance associated with these tissues, DAMs were mapped to the Kyoto Encyclopedia of Genes and Genomes (KEGG) database (<http://www.genome.jp/kegg/>). More pathways were impacted in downregulated DAMs as compared with upregulated DAMs (Fig. 4 and Supplementary Table S2). Secondary metabolism and polyunsaturated fatty acid (PUFA) metabolism pathways were significantly enriched in both up- and downregulated DAMs (adj. P -value < 0.001) (Fig. 4). In the

downregulated DAMs, the following pathways were enriched (adj. P -value < 0.001): arachidonic acid metabolism; α -linolenic acid metabolism; linoleic acid metabolism; flavone and flavonol biosynthesis; tropane, piperidine, and pyridine alkaloid biosynthesis; and phenylpropanoid biosynthesis (Fig. 4a). The α -linolenic acid metabolism pathway was also significantly enriched among upregulated DAMs, along with sesquiterpenoid biosynthesis pathway as well as limonene and pinene degradation pathways (adj. P -value < 0.001) (Fig. 4b). In addition to PUFA and secondary metabolism pathways, amino acid biosynthesis and metabolism pathways were also enriched in downregulated DAMs (adj. P -value < 0.05), with phenylalanine metabolism being significantly enriched in the downregulated DAMs (adj. P -value < 0.001) (Fig. 4a).

Annotation of Female versus Male Flower DAMs

Annotations of unknown floral tissue metabolites were assigned using *Compound Discoverer* software (CD) from consensus evaluation based on elemental composition prediction, spectral library (mzCloud) and database (ChemSpider) searches, as well as the database ranking algorithmic tool mzLogic. Of the 626 downregulated and 861 upregulated putative compounds (1487 compounds in total), 41 compounds that represented 2.8% of the total number of DAMs were assigned annotations based on the consensus evaluation. There were 19 compounds annotated in the upregulated group (Table 2), with 22 compounds in the downregulated group (Table 3).

Of the 19 upregulated compounds in female versus male floral tissues, 10 compounds were initially annotated as the cannabidiol (CBD) hydroxyquinone HU-331 (compounds 25, 28, 29, 31, 32, 33, 35, 38, 39, and 41 in Table 2). One compound in the downregulated group (compound 34 in Table 3), was also initially annotated as HU-331. These 11 HU-331-annotated compounds all had a calculated molecular mass of 328.2039 based on MS data, which matches the molecular formula of $C_{21}H_{28}O_3$. The different retention times of putative HU-331-annotated compounds ranged from 9.1 to 14.6 min and indicated that these compounds are molecular isomers.

Fragment Ion Search (FISH) coverage score, an algorithmic measurement of the percentage of MS^2 ions which match *in silico* fragmentation patterns based on literature-defined chemical reactions from the HighChem Fragmentation Library, was applied to the HU-331 annotated compounds in an attempt to further discriminate the compounds from one another. FISH coverage scores of HU-331-like compounds varied from 38.46% to 94.74% (Tables 2 and 3), with higher FISH scores being more supportive of the annotated chemical structure. Compound 32 with retention time of 11.4 min gave the highest FISH score of 94.7% among the 11 similarly annotated compounds, indicating that this compound is likely to be HU-331. The MS^2 spectrum of compound 32 (Supplementary Material, Appendix S1) gave a base peak of m/z 329.2108 that corresponded to the $[M + H]^+$ ion. Upon comparison of its MS^2 spectrum to that of HU-331 from the mzCloud reference library, it became apparent that the fragmentation patterns and their calculated elemental composition did not match, indicating that compound 32 could be a structural isomer of HU-331. The MS^2 spectra of the other compounds with the same pseudo-molecular ions were also extracted (Supplementary Material, Appendix S1) and compared with that of HU-331 (Supplementary Material, Appendix S2). Compounds 28, 29, 31, 32, and 33 showed the presence of fragment ion m/z 311.201, which corresponds to

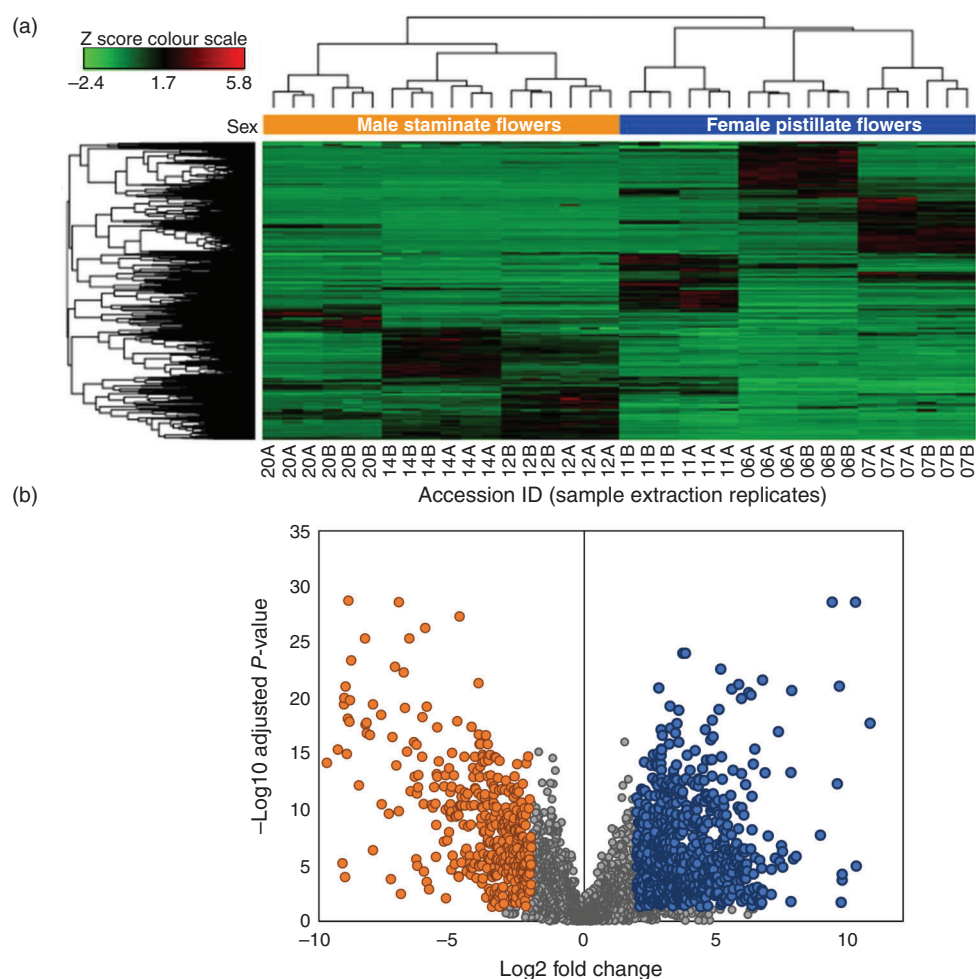


Fig. 3. Comparison of metabolite abundances between female versus male floral samples. (a) Two-way hierarchical cluster analysis (HCA) and heat map using metabolite chromatographic peak areas of male and female floral tissue samples. Cluster analysis performed on putative metabolites identified from male and female floral tissue samples. Values scaled before clustering and Euclidean distance was used for cluster analysis. *Numbers* represent accession IDs (Table 1); A, apical inflorescence; B, basal inflorescence. (b) Volcano plot of 2599 differentially abundant putative metabolites identified from male and female floral tissue samples. Orange dots and blue dots represent metabolites characteristic of male and female floral tissues, respectively (P -value = 0.05 ($-\log_{10} 0.05 = 1.3$), \log_2 fold change = 2). Grey dots represent metabolites that are not significantly different between the female and male groups.

a loss of a water molecule and is indicative of the presence of a hydroxy substituent in the molecule. Compound **25** that eluted at 9.1 min showed a different MS^2 spectrum compared with the other compounds, suggesting that this compound could be of a different class to that of the other 10 unknown compounds. Compound **35** at 12.8 min also showed greater variation in the fragment ions which also differentiated this compound from the others. Compounds **38**, **39**, **41**, and **34** all showed a base peak at m/z 229.086 that matched the fragment ion of HU-331 with a chemical formula of $C_{14}H_{13}O_3^+$ for the benzoquinone moiety with alkene sidechain as shown in the mzCloud reference library (Supplementary Material, Appendix S2). The four compounds **38**, **39**, **41**, and **34**, and compounds **28**, **29**, **31**, **32**, and **33** showed some similarity of fragment ions with that of HU-331 and most probably represent two groups of hydroxy-benzoquinones with different substituents.

Compound **40**, corresponding to the molecular formula $C_{22}H_{30}O_4$ and $[M + H]^+$ ion at m/z 358.21434, was incorrectly annotated as cannabidiolic acid by the CD software. Despite being identified as CBDA across multiple annotation sources,

this compound eluted 2.9 min after the CBDA reference standard and had a low FISH coverage score of 42.96 % (Table 2). This compound was an upregulated DAM in the female flowers and was subsequently identified as Δ^9 -tetrahydrocannabinolic acid A (Δ^9 -THCAA), with the nominal mass (Δ ppm < 5) as well as retention time matching that of the Δ^9 -THCAA reference standard at 14.6 min.

Analogous with the KEGG pathway enrichment analysis, several lipid and flavonoid metabolites were identified through consensus evaluation from DAMs of the female versus male floral tissues. Lipid constituents with FISH coverage scores ≥ 75 % included α -linolenic acid, 9-oxo-octadecadienoic acid (ODE), tetranor-12(*R*)-HETE in the downregulated group, and 12-oxo-phytodienoic acid in the upregulated group (Fig. 5 and Tables 2 and 3). Two PUFA-derived endocannabinoid-like acylethanolamides, palmitoyl ethanolamide and α -linolenoyl ethanolamide, were also observed in the downregulated DAMs, with FISH coverage scores of these metabolites being greater than 90 %. The flavonoids apigenin, apigenin 7-O-glucuronide, diosmetin, and oroxindin were identified in the upregulated

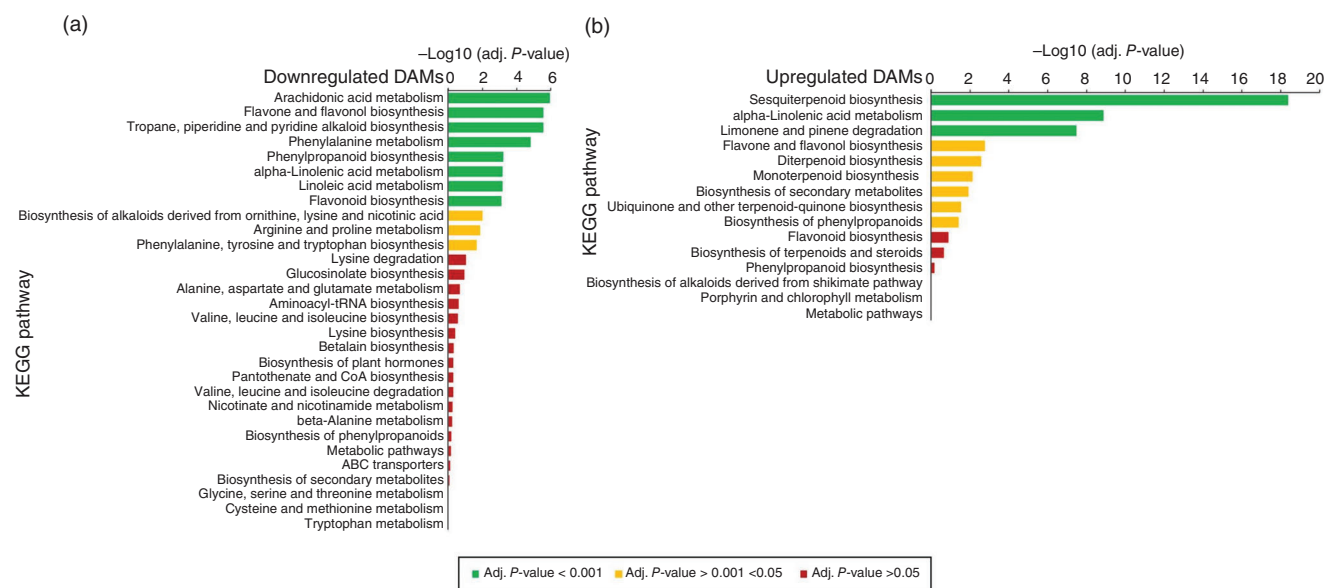


Fig. 4. KEGG enrichment of differentially regulated metabolic pathways in female versus male floral tissues. (a) KEGG enrichment of metabolic pathways for downregulated differentially abundant metabolites (DAMs) in female versus male floral tissues. (b) KEGG enrichment of metabolic pathways for upregulated DAMs in female versus male floral tissues. Kyoto Encyclopedia of Genes and Genomes (KEGG; website: <https://www.genome.jp/kegg/pathway.html>) pathway enrichment *P*-values were calculated using the Metabolites Biological Role (MBRole) server^[69] and adjusted for multiple testing using the Benjamini–Hochberg correction for the false-discovery rate.^[70] KEGG pathways ranked in order of adjusted *P*-value. Only the top 30 KEGG pathways relevant to plant metabolism were plotted from each differential metabolite group.

group (Fig. 5 and Table 2), while kaempferol-3-glucoside-7-rhamnoside, orientin, quercetin, and quercetin-3-β-D-glucoside were identified in the downregulated group (Fig. 5 and Table 3). Of these, only quercetin, oxroindin, and diosmetin had FISH coverage scores $\geq 75\%$ (Tables 2 and 3).

Quantitative Analysis of Phytocannabinoids

Fourteen phytocannabinoids, for which certified reference standards are available, were determined quantitatively from the male and female floral tissues of six *Cannabis* accessions and the results are summarised in Table 4. Given that the plants used for metabolomic analysis were derived from industrial hemp varieties, it was anticipated that CBDA/CBD, which are commonly associated with such germplasm, would be the predominant phytocannabinoids among the floral samples. CBDA concentration was observed to be highest in accessions 06 and 11 (554.53 to 798.10 mg/100 g), and its decarboxylated form CBD was highest in accession 11 (901.29 mg/100 g in the apical floral tissue), which was evident in the representative TICs of the accessions in Fig. 2 (compounds 42 and 43, respectively). Surprisingly, the profile of accession 07 was high in Δ9-THCAA (1254.30 and 653.86 mg/100 g for apical and basal floral tissues, respectively) and Δ9-THC (1481.90 and 1350.29 mg/100 g for apical and basal floral tissues, respectively) compared with other accessions and these compounds were the predominant phytocannabinoids in the profile of this plant. The total THC content of two individual plants derived from accessions 06 and 07 exceed the limit set under the provisions of the Drugs, Poisons and Controlled Substances Act 1981. These plants were subsequently destroyed during harvest and were not used for further propagation.

Another indication of the chemical diversity of plants used for comparative metabolomic analysis was the unusual chemotype of the female plant from accession 06 which showed elevated levels of what are typically minor alkyl phytocannabinoid homologues. CBDVA and THCVA, which differ from CBDA and Δ9-THCAA,

respectively, by the number of carbon atoms on their alkyl side chains, exhibited variable concentration among the accessions with accession 06 having the highest concentration. As expected, a similar trend was observed for the corresponding decarboxylated forms, with CBDV and THCV highest in accession 06. CBNA and CBN, which are oxidation artefacts of Δ9-THCAA and THC, respectively,^[6] had relatively low concentrations among the floral samples examined. Interestingly, the concentration of the juvenile cannabinoid CBCA was 5–20-fold higher in the female plants from accessions 06, 07, and 11 (431.52 to 719.86 mg/100 g) compared with the male plants from accessions 12, 14, and 20 (19.60 to 126.31 mg/100 g). CBGA, which is the precursor of CBDA, Δ9-THCAA, and CBCA,^[6] exhibited a concentration range of > 30 fold (0.71 to 32.35 mg/100 g) for the six accessions.

The decarboxylated phytocannabinoids are generated from their respective carboxylated forms either *in planta*, post-harvest (upon exposure to, for example, light and/or heat), or both. The floral samples exhibited varying levels of decarboxylation among the phytocannabinoid species examined (e.g. CBD/CBDA and THC/THCA), although a higher Δ9-THC concentration than its acid form (Δ9-THCAA) is evident for all floral tissue samples. A similar trend of higher CBD concentration can be observed within accessions 11, 12, 14, and 20 but the reverse is true for accessions 06 and 07.

In addition to variation in the relative abundance of phytocannabinoids among male and female plants, variation in the total cannabinoid content was also evident from the targeted analysis of phytocannabinoids (Fig. 6a). To assess the relative proportion of each phytocannabinoid species in the samples, the concentration of the acid and decarboxylated forms were combined (e.g. CBD + CBDA, Δ9-THCAA + Δ9-THC, etc; Fig. 6b). The analysis of the apical and basal floral tissues from the six accessions generally did not exhibit a large variation in the phytocannabinoid concentration within the accession, although a trend of slightly higher levels in the apical inflorescence can be

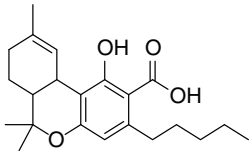
Table 2. Annotation assignments of upregulated metabolites in female versus male flowers from consensus evaluation

Consensus evaluation based on elemental composition prediction, mzCloud and ChemSpider searches, as well as the mzLogic algorithmic ranking tool

Tentative compound identification	Chemical structure	Chemical formula	Molecular weight	RT [min]	FISH coverage
15 Apigenin 7- <i>O</i> -glucuronide		C ₂₁ H ₁₈ O ₁₁	446.0848	7.0	50.00
16 Coumaroyl-tyramine isomer I		C ₁₇ H ₁₇ NO ₃	283.1208	7.3	100.00
17 Coumaroyl-tyramine isomer II		C ₁₇ H ₁₇ NO ₃	283.1209	7.6	83.33
18 Oroxindin		C ₂₂ H ₂₀ O ₁₁	460.1005	8.0	100.00
19 9 <i>S</i> ,13 <i>R</i> -12-Oxophytodienoic acid		C ₁₈ H ₂₈ O ₃	292.2039	8.4	80.00
20 Apigenin		C ₁₅ H ₁₀ O ₅	270.0528	8.6	43.75
23 Diosmetin		C ₁₆ H ₁₂ O ₆	300.0634	8.7	87.50
25 Unknown	HU-331 analogue (Supplementary Material Appendix S2)	C ₂₁ H ₂₈ O ₃	328.2039	9.1	75.00
26 Caryophyllene oxide		C ₁₅ H ₂₄ O	220.1827	9.4	70.59
28 Unknown	HU-331 analogue (Supplementary Material Appendix S2)	C ₂₁ H ₂₈ O ₃	328.2039	10.4	76.00
29 Unknown	HU-331 analogue (Supplementary Material Appendix S2)	C ₂₁ H ₂₈ O ₃	328.2039	10.8	84.62
31 Unknown	HU-331 analogue (Supplementary Material Appendix S2)	C ₂₁ H ₂₈ O ₃	328.2039	11.2	73.91
32 Unknown	HU-331 analogue (Supplementary Material Appendix S2)	C ₂₁ H ₂₈ O ₃	328.2039	11.4	94.74
33 Unknown	HU-331 analogue (Supplementary Material Appendix S2)	C ₂₁ H ₂₈ O ₃	328.2039	11.7	84.21

(continued)

Table 2. (Continued)

Tentative compound identification	Chemical structure	Chemical formula	Molecular weight	RT [min]	FISH coverage
35 Unknown	HU-331 analogue (Supplementary Material Appendix S2)	C ₂₁ H ₂₈ O ₃	328.2039	12.8	58.33
38 Unknown	HU-331 analogue (Supplementary Material Appendix S2)	C ₂₁ H ₂₈ O ₃	328.2039	13.9	38.46
39 Unknown	HU-331 analogue (Supplementary Material Appendix S2)	C ₂₁ H ₂₈ O ₃	328.2039	14.0	39.06
40 Δ ⁹ -tetrahydrocannabinolic acid		C ₂₂ H ₃₀ O ₄	58.2143	14.6	42.96
41 Unknown	HU-331 analogue (Supplementary Appendix S2)	C ₂₁ H ₂₈ O ₃	328.2039	14.6	62.50

observed, especially among the female floral samples. Accession 06 gave the highest total phytocannabinoid concentration (5427.69 and 4964.72 mg/100 g for apical and basal floral tissues, respectively) with CBDVs and THCVs as the more dominant phytocannabinoids within the accession. The total phytocannabinoid concentration for the other accessions varied with accession 07 > accession 11 > accession 20 > accession 14 > accession 12. From these data it can be observed that the average total concentration of phytocannabinoids from floral tissues of female plants (accessions 06, 07, and 11) are higher compared with those of the male plants (accessions 12, 14, and 20) as shown in Fig. 6c.

Discussion

The Metabolome of Cannabis Flowers

While the use of genomic and transcriptomic resources to elucidate molecular mechanisms underlying trait diversity in *Cannabis* has accelerated in recent years,^[30] our understanding of the abundance and diversity of chemical constituents defining chemotypic groups is lacking.^[29] Metabolomic information can provide greater resolution of underlying biological processes than is possible with other omics-based analyses as metabolites represent the endpoint of cellular process and are therefore more proximal to the phenotype or chemotype under investigation.^[31] Identifying a set of metabolites that distinguishes samples from two or more groups is reliant on both a comparison of a sufficient number of samples to obtain statistically meaningful information as well as on the ability of these samples to adequately capture biological variation so as to avoid spurious associations.^[31,32] In the absence of pilot data to inform experimental design, extracting relevant and interpretable information from metabolic datasets remains challenging.^[31,33] To maximise group variation, biological replicates used in the comparison of male and female *Cannabis* flowers were selected at the level of accession (variety). Multivariate analysis showed that the biological replicates of each accession clustered in distinct spaces indicating that the impact of sexual phenotype was substantial and specific, despite the limited sample size (Fig. 1b and Fig. 3a).

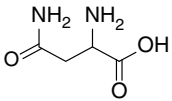
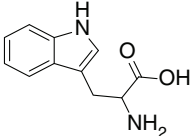
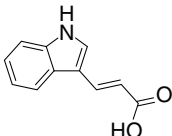
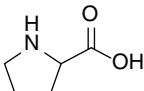
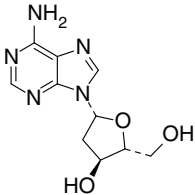
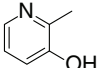
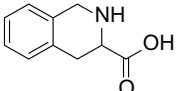
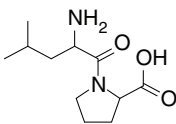
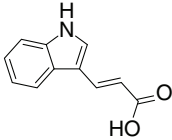
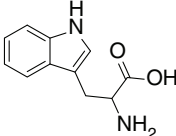
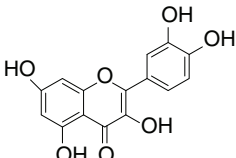
Another obstacle which complicates interpretation of metabolomic variation between chemotypes is identifying the vast catalogue of small molecules present within samples.^[29,34] Annotation assignments of unknown floral metabolites was performed in *Compound Discoverer* software by consensus evaluation of elemental composition prediction, database, and MS² spectral library searches. These integrated approaches increase the level of confidence in the annotation of metabolites from the available HRMS information, although this level of stringency ultimately reduces the number of reportable compounds. Of the 2599 compounds identified across floral samples, only 211 or ~8% of all compounds had a full match with the vendor-specific spectral library (mzCloud), compared with 936 compounds which matched ChemSpider database searches and 2382 compounds with predicted elemental compositions matching theoretical isotope patterns. While there are varying levels of identification rigour which can be applied to the reporting of compounds from untargeted metabolomic analyses (varying from unambiguous identification to compound classes and unclassified metabolites),^[35] a major bottleneck in the confidence of compound annotation is matching MS² fragments with library spectra fragments. Development of customised MS² spectral libraries, such as those applied to *Cannabis sativa* var. Kompolti for phenolic compound identification,^[29] coupled with the acquisition of high-quality HRMS fragmentation data is anticipated to improve annotation of unknown compounds and allow for more detailed profiling of phenotypic variation in *Cannabis*. Application of these spectral libraries within untargeted metabolomic analysis pipelines will also be a critical step in understanding the complexity of botanical formulations derived from *Cannabis*.

Phytocannabinoid Variation Among Floral Samples

Our analysis among six accessions showed that cannabinoid contents were consistently higher in the female samples as compared with male flowers (Fig. 6c). Previous analyses of cannabinoid contents among unisexual plants yielded inconsistent results, with comparisons either showing no differences between male and female inflorescences or showing a higher cannabinoid content in female floral tissues.^[25–28] This could be attributed to several factors.

Table 3. Annotation assignments of downregulated metabolites in female versus male flowers from consensus evaluation

Consensus evaluation based on elemental composition prediction, mzCloud and ChemSpider searches, as well as the mzLogic algorithmic ranking tool

Tentative compound identification	Chemical structure	Chemical formula	Molecular weight	RT [min]	FISH coverage
01 Asparagine		C ₄ H ₈ N ₂ O ₃	132.0535	1.0	25.00
02 Tryptophan		C ₁₁ H ₁₂ N ₂ O ₂	204.0898	1.2	100.00
03 Indole-3-acrylic acid		C ₁₁ H ₉ NO ₂	187.0633	1.2	70.00
04 Proline		C ₅ H ₉ NO ₂	115.0633	1.2	100.00
05 2'-Deoxyadenosine		C ₁₀ H ₁₃ N ₅ O ₃	251.1017	1.3	66.67
06 3-Hydroxy-2-methylpyridine		C ₆ H ₇ NO	109.0528	1.3	33.33
07 Tetrahydroisoquino-line-3-carboxylic acid		C ₁₀ H ₁₁ NO ₂	177.0789	1.4	66.67
08 Leucylproline		C ₁₁ H ₂₀ N ₂ O ₃	228.1473	1.8	72.22
09 Indole-3-acrylic acid		C ₁₁ H ₉ NO ₂	187.0633	2.0	88.24
10 Tryptophan		C ₁₁ H ₁₂ N ₂ O ₂	204.0898	2.0	94.44
11 Quercetin		C ₁₅ H ₁₀ O ₇	302.0427	6.3	76.00

(continued)

Table 3. (Continued)

Tentative compound identification	Chemical structure	Chemical formula	Molecular weight	RT [min]	FISh coverage
12 Orientin		C ₂₁ H ₂₀ O ₁₁	448.1005	6.4	42.86
13 Kaempferol-3-glucoside-7-rhamnoside		C ₂₇ H ₃₀ O ₁₅	594.1586	6.4	55.56
14 Quercetin-3β-D-glucoside		C ₂₁ H ₂₀ O ₁₂	464.0954	6.6	50.00
21 9-Oxo-10E,12Z-octadecadienoic acid		C ₁₈ H ₃₀ O ₃	294.2195	8.7	74.36
22 Sedanolid		C ₁₂ H ₁₈ O ₂	194.1306	8.7	34.29
24 Tetranor-12(R)-HETE		C ₁₆ H ₂₆ O ₃	266.1881	8.7	81.48
27 Anwulignan		C ₂₀ H ₂₄ O ₄	328.1674	9.4	50.00
30 α-Linolenoyl ethanolamide		C ₂₀ H ₃₅ NO ₂	321.2668	11.2	93.75
34 Unknown	HU-331 analogue (Supplementary Material Appendix S2)	C ₂₁ H ₂₈ O ₃	328.2038	12.1	50.00
36 Palmitoyl ethanolamide		C ₁₈ H ₃₇ NO ₂	299.2824	13.0	100.00
37 α-Linolenic acid		C ₁₈ H ₃₀ O ₂	278.2246	13.3	85.71

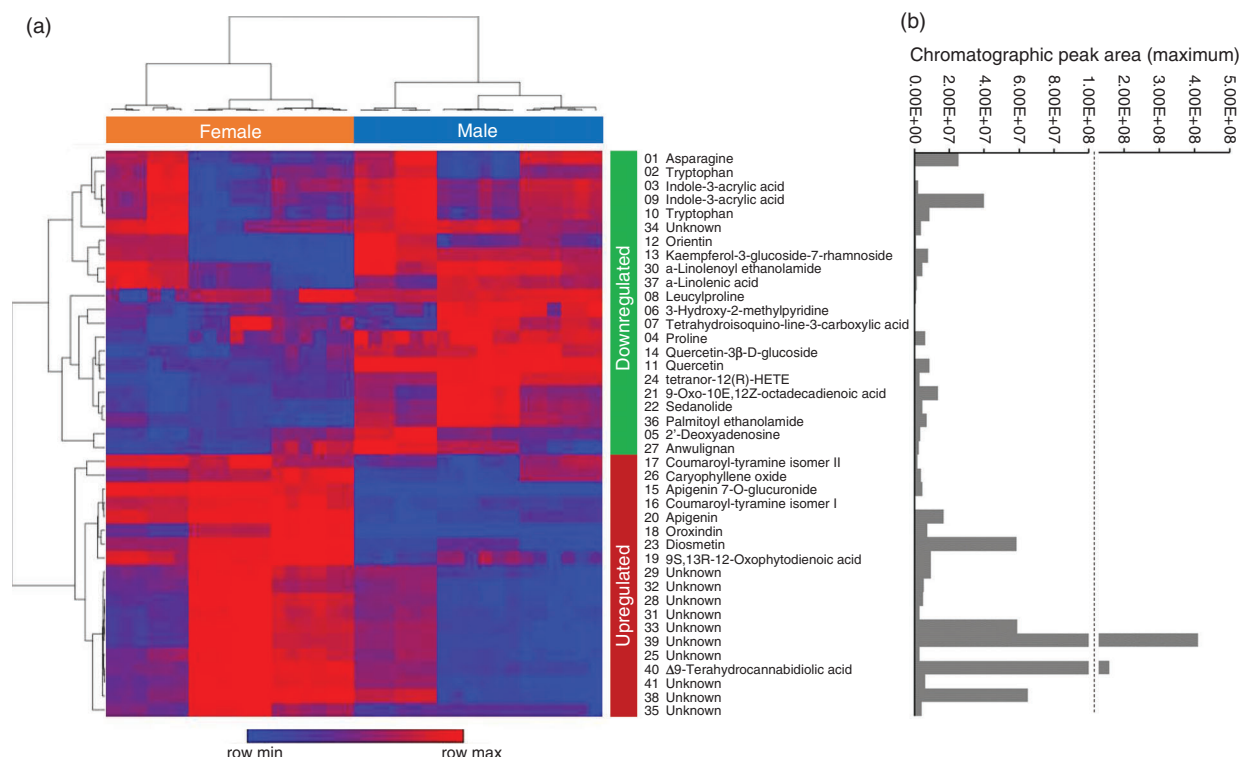


Fig. 5. Relative abundance and chromatographic peak area intensities of DAMs. (a) Two-way hierarchical cluster analysis (HCA) and heat map of female versus male annotated DAMs. One minus Pearson correlation used for cluster analysis. HCA and heat map drawn using the Broad Institute's Morpheus visualisation and analysis software (Morpheus, <https://software.broadinstitute.org/morpheus/>). Heat map relative colour scheme uses minimum and maximum \log_{10} chromatographic peak area values from each row. (b) Largest chromatographic peak areas of the 41 annotated DAMs. Annotation of DAMs performed using consensus evaluation of elemental composition prediction, mzCloud and ChemSpider searches as well as the mzLogic algorithmic ranking tool. Chromatographic peak areas represent the maximum area across all floral samples analysed. Group peak areas can be found in Supplementary Table S3.

One possible source of variation contributing to inconsistencies in phytocannabinoid content among unisexual flowers could relate to the sampling of floral tissues. Male inflorescences are largely comprised of staminate flowers and have a low abundance of vegetative tissue, with glandular trichomes, which are the major site for phytocannabinoid synthesis and accumulation, concentrated on the surface of anthers.^[12,15,36] In contrast, female inflorescences have a more complex highly branched heterogeneous structure where trichome abundance is concentrated on a subset of vegetative tissues, such as the perigonal bracts, surrounding flowers (see Fig. 1a).^[14,36]

Previous comparisons between unisexual flowers have not discriminated between inflorescence component tissues such as low-phytocannabinoid containing foliage leaves and those directly encasing the carpel and pistillate flowers, while others have homogenised inflorescences bearing immature fruit (seed).^[26–28] These details are especially relevant given the variation in female plant architecture and inflorescence structure reported among sub-taxa, such as variation in branching, internode length, and bract abundance.^[14] Congruent with the cluster analysis, four of the six accessions showed a higher cannabinoid content in the apical inflorescence as compared with basal inflorescence samples (Fig. 6a), indicating that the age and tissue-type of the plant material sampled will also impact comparative analyses among unisexual flowers. As with other aspects of chemotype identified in female plants, such as proportion and content of phytocannabinoids,^[11,37] genotype-specific variation could also be contributing to patterns of cannabinoid content among unisexual flowers.

DAMs Associated with Sexual Phenotype

While incorrectly annotated as CBDA by *Compound Discoverer* software due to the absence of Δ^9 -THCAA MS² fragmentation data in the available spectral libraries, independent identification of one of the predominant phytocannabinoids segregating between male and female floral samples indicates that the DAMs identified from untargeted metabolomic analysis are biologically meaningful and specific to the sexual phenotypes under investigation (Fig. 2 and Fig. 5). In addition to identifying phytocannabinoid variation, our untargeted analysis of unisexual flowers also revealed several metabolites known to be involved in pollen sterility to be among the male-specific DAMs.

Consistent with other analyses of male flowers and pollen-producing tissues,^[38–40] several pathways relating to PUFA metabolism as well as flavone and flavonol biosynthesis were enriched in the downregulated (male-specific) DAMs (Fig. 4). It is well established that flavonoids play a key role in pollen viability.^[38] Flavonols, as opposed to other flavonoids produced in the anthers of the flower, such as quercetin and kaempferol, promote pollen fertility and pollen tube growth in vitro.^[38] Analysis of transgenic plants with reduced chalcone synthase gene expression have resulted in abnormal anthers with impaired pollen tube growth and low germination efficiency in *Petunia* and *Solanum*, respectively.^[39,40] In agreement with previous HPLC-DAD-MSⁿ analysis comparing quercetin di-C-hexoside between male and female *Cannabis sativa* var. Spontanea flowers,^[25] our analysis shows quercetin to be predominantly present in the male sexual phenotype with only

Table 4. Cannabinoid concentration of *Cannabis* apical and basal floral tissues from six accessions
Compound number annotated in Fig. 2 indicated in brackets. Values are reported as average of three replicates \pm standard deviation. ND, not detected

Sex	Acc.	ID	Analyte concentration, mg/100 g																THCV (54)
			CBDA (42)	CBD (43)	Δ9-THCAA (40)	Δ9-THC (44)	CBCA (45)	CBC (46)	CBGA (47)	CBG (48)	CBNA (49)	CBN (50)	CBDVA (51)	CBDV (52)	THCVA (53)				
F	06	Apical	798.10 ± 18.18	263.61 ± 15.89	292.14 ± 3.28	392.24 ± 13.14	719.86 ± 51.57	42.31 ± 1.16	32.34 ± 2.65	15.48 ± 0.95	8.49 ± 0.83	7.08 ± 0.28	1325.32 ± 60.62	214.79 ± 2.05	780.01 ± 14.77	535.93 ± 9.08			
		Basal	725.54 ± 33.44	261.46 ± 8.86	246.90 ± 24.17	361.33 ± 5.62	613.84 ± 47.44	35.76 ± 1.10	30.00 ± 1.87	15.19 ± 0.96	10.68 ± 0.14	8.72 ± 0.57	1139.02 ± 136.46	192.23 ± 10.27	849.99 ± 3.04	474.04 ± 11.67			
F	07	Apical	7.24 ± 0.60	3.51 ± 0.10	1254.30 ± 110.24	1481.90 ± 18.96	557.15 ± 51.31	52.01 ± 2.60	32.35 ± 2.84	25.18 ± 1.17	25.89 ± 0.82	25.60 ± 1.14	ND	0.09 ± 0.01	17.75 ± 0.52	8.57 ± 0.16			
		Basal	6.11 ± 0.26	3.88 ± 0.05	653.86 ± 54.17	1350.29 ± 72.49	431.52 ± 40.21	55.73 ± 4.28	25.57 ± 1.47	26.18 ± 0.37	16.18 ± 0.68	22.49 ± 1.14	1.13 ± 0.07	0.20 ± 0.01	13.94 ± 0.14	8.87 ± 0.35			
F	11	Apical	728.20 ± 50.72	901.29 ± 22.67	9.54 ± 0.83	59.06 ± 2.01	670.37 ± 101.98	163.70 ± 8.62	5.17 ± 0.43	6.84 ± 0.37	3.15 ± 0.18	1.89 ± 0.13	122.61 ± 5.47	43.73 ± 1.29	3.63 ± 0.27	4.98 ± 0.10			
		Basal	554.53 ± 4.84	661.07 ± 11.52	9.70 ± 0.31	39.13 ± 0.71	612.18 ± 19.40	86.29 ± 3.47	4.37 ± 0.22	3.57 ± 0.12	4.83 ± 0.30	1.52 ± 0.03	108.83 ± 2.77	32.14 ± 1.61	3.59 ± 0.20	3.42 ± 0.13			
M	12	Apical	98.95 ± 3.89	206.94 ± 3.53	0.33 ± 0.02	14.15 ± 0.27	23.46 ± 0.50	29.70 ± 0.23	0.75 ± 0.05	0.25 ± 0.02	ND	0.22 ± 0.01	3.67 ± 0.17	3.51 ± 0.09	ND	0.36 ± 0.01			
		Basal	111.91 ± 10.44	241.23 ± 16.25	0.57 ± 0.01	15.97 ± 0.34	22.18 ± 1.82	34.87 ± 0.33	0.71 ± 0.06	0.48 ± 0.03	ND	0.28 ± 0.03	4.79 ± 0.25	4.88 ± 0.11	ND	0.47 ± 0.03			
M	14	Apical	196.25 ± 17.93	409.28 ± 13.26	1.06 ± 0.04	28.43 ± 0.63	19.60 ± 0.91	25.30 ± 0.42	1.91 ± 0.12	2.21 ± 0.06	ND	0.48 ± 0.03	4.65 ± 0.38	5.87 ± 0.23	ND	0.59 ± 0.02			
		Basal	238.74 ± 14.99	448.19 ± 15.37	1.28 ± 0.04	28.33 ± 0.42	24.92 ± 1.38	27.70 ± 0.84	2.52 ± 0.08	3.17 ± 0.03	ND	0.51 ± 0.02	4.58 ± 0.16	6.19 ± 0.02	ND	0.62 ± 0.02			
M	20	Apical	467.32 ± 7.91	515.61 ± 14.47	25.21 ± 2.35	358.09 ± 7.10	120.12 ± 3.33	89.61 ± 4.19	1.37 ± 0.04	5.82 ± 0.26	0.73 ± 0.05	4.72 ± 0.10	19.14 ± 0.44	12.97 ± 0.18	5.17 ± 0.38	24.41 ± 0.06			
		Basal	318.04 ± 7.11	394.31 ± 5.92	20.76 ± 1.65	281.91 ± 6.94	126.31 ± 12.54	71.90 ± 3.29	1.62 ± 0.14	8.20 ± 0.25	0.90 ± 0.09	4.03 ± 0.04	19.23 ± 0.16	10.34 ± 0.14	5.99 ± 0.25	20.18 ± 0.20			

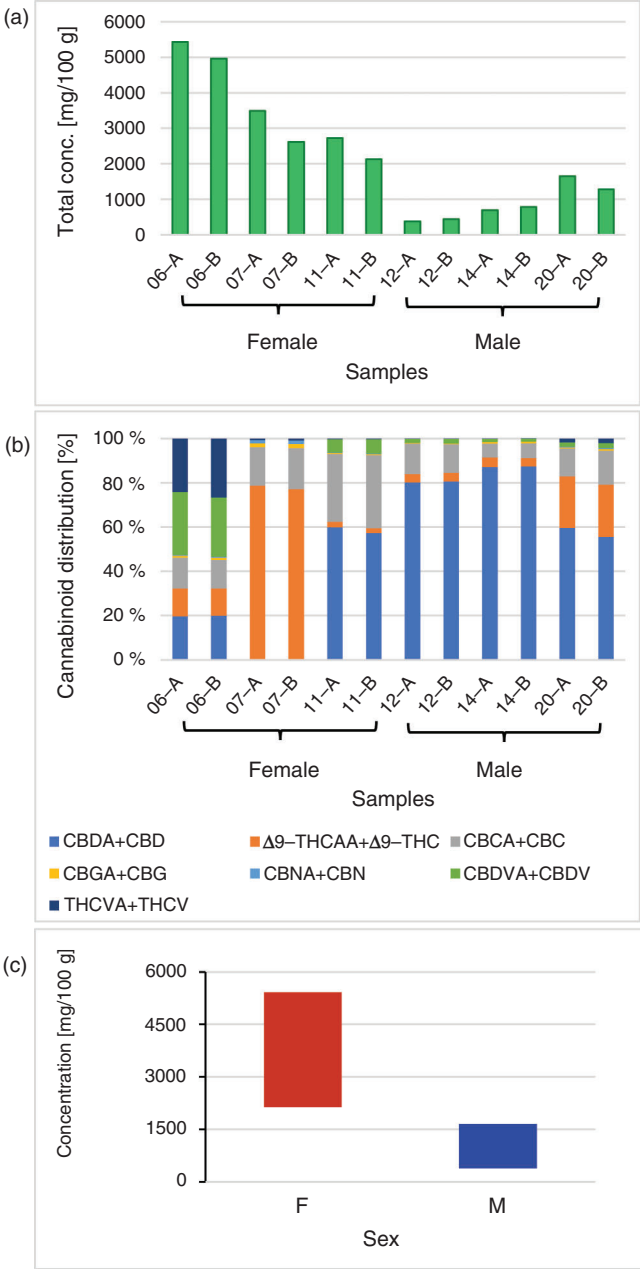


Fig. 6. Phytocannabinoid concentrations in male and female floral tissue samples from six *Cannabis* accessions. (a) Comparison of total cannabinoid concentration among *Cannabis* accessions. (b) Percentage distribution of cannabinoids in each accession. (c) Range of values of total cannabinoid concentration between female and male floral tissues from six *Cannabis* accessions.

trace levels detected in female floral samples (Fig. 5). While the mechanism underlying flavonoid accumulation and pollen fertility remain unclear, quercetin and possibly other flavones identified to be upregulated in male floral tissues may participate in reactive oxygen species (ROS) homeostasis in anthers, thereby limiting ROS-facilitated pollen abortion.^[41] As with the flavonoid pathways, over-representation of linoleic and α -linolenic pathways in pollen producing tissues is not uncommon. Stearoyl-ACP desaturase, ER desaturases (FAD3, FAD2), and FATB thioesterases involved in the termination of C₁₆ fatty acids are differentially expressed in male flowers, and linolenic

acid as well as linoleic acid are the predominant constituents in the lipid fractions of pollen.^[42–44]

While the α -linolenic acid metabolism pathway was impacted by DAMs specific to both male and female flowers, this pathway could be utilised differently between unisexual flowers, with the untargeted analysis of floral tissues indicating that the jasmonate (JA) pathway may play a role in flower development and secondary metabolism in female plants. Among the upregulated differential metabolites, one fatty acyl octadecanoid with the molecular formula $C_{18}H_{28}O_3$ and $[M + H]^+$ ion at m/z 292.2039 was identified via consensus evaluation as 12-oxo-phytodienoic acid (OPDA) (Fig. 5 and Table 2). OPDA is a linolenic acid-derived oxylipin signalling molecule and a direct precursor to JA.^[45] JA, jasmonoyl-L-isoleucine, and methyl JA, collectively known as jasmonates, regulate gene expression governing plant developmental, physiological, and defence processes and are directly implicated in flower development, seed maturation, and induction of plant defence compounds such as various terpenoids.^[46,47]

Despite OPDA being biosynthetically related to JA, it has a distinct role in signalling and gene transcription independent of other jasmonates. Of relevance to sexual phenotype in *Arabidopsis* are upregulated OPDA-specific genes associated with auxin (At3g09870, At5g35735) and abscisic acid (ABA) (At5g13200) hormonal responses.^[46] OPDA is the dominant oxylipin in seed coat tissues of various plant species, and female-sterility in JA-insensitive mutants can be rescued by wound-induction synthesis of OPDA, indicating OPDA-specific regulation of embryo development.^[45,48,49] OPDA also shows synergistic effects with ABA, increases ABA INSENSITIVE5 protein abundance, and its concentration is affected by ABA via the proposed action of PLASTID LIPASE2 and 3.^[50] In *Cannabis*, ABA can fully inhibit GA induction of male flowers in female plants and indole-3-acetic acid (IAA) induction of female flowers in male plants.^[20,51] Two compounds corresponding to the molecular formula $C_{11}H_9NO_2$ and $[M + H]^+$ ion at m/z 187.0633 were identified as indole-3-acrylic acid (IAcRA) in the down-regulated DAMs (Table 3 and Fig. 5), although the function of this auxin is primarily associated with plant growth metabolic processes.^[52]

Irrespective of florogenesis, the upregulation of jasmonates, such as OPDA, in the high phytocannabinoid yielding female floral samples may indicate a possible role for oxylipin signalling in *Cannabis* secondary metabolism. Congruent with this hypothesis is the enrichment of monoterpenoid and sesquiterpenoid pathways as well as the annotation of sesquiterpene caryophyllene oxide in the female flowers (Fig. 4b and Table 2). Changes in THC, CBD, and carotenoid content have been reported in *Cannabis* vegetative tissues treated with between 1 and 100 μ M JA,^[53] while application of ABA increases THC content in female and male floral tissues.^[54] There are four stereoisomers of OPDA, with the natural *cis* isomer (9*S*,13*S*)-OPDA being relevant in JA biosynthesis. The OPDA upregulated in female flowers was identified across annotation sources as the *trans* isomer (9*S*,13*R*)-OPDA (Table 2). However, it is not possible to discriminate these isomers with the LC stationary phase used in this study. This is the first report of the upregulation of OPDA in *Cannabis* flowers and given that APA- and auxin-related genes are directly implicated in sex expression,^[20,51,55] this compound may represent a molecule of interest for further investigation.

Unknown Phytocannabinoid-Like DAMs in *Cannabis* Flowers

Eleven compounds were identified as molecular isomers of HU-331 corresponding to the molecular formula $C_{21}H_{28}O_3$ and $[M + H]^+$ ion at m/z 329.2115; 10 of which were upregulated in the female floral samples (Fig. 5 and Table 2). In addition to differing by retention time, the MS² spectra of these compounds showed differences in their fragmentation patterns and suggested three different groups or classes with compounds 25 and 35 differing from each other and the other molecular isomers. The other compounds 28, 29, 31, 32, 33, 34, 38, 39, and 41 showed several fragment ions that were similar to the fragment ions of HU-331, although some of the elemental compositions did not match that of HU-331 when calculated within 5 ppm of the observed masses. However, the MS² spectra of these nine compounds indicated that these could be structural isomers of a hydroxybenzoquinone-type compound with different substituents.

Some benzoquinones can be synthesised non-enzymatically from phytocannabinoids. Examples are HU-331,^[56] HU-336,^[57] HU-345,^[57] and VCE-003^[58] from the oxidation of CBD, Δ^8 -THC, CBN, and CBG, respectively. Upregulation of multiple phytocannabinoid derivatives may be suggestive of a greater flux through the phytocannabinoid pathway in female flowers as compared with the male flowers which is consistent with the higher phytocannabinoid content identified in the female floral samples. HU-331 represents a potential anti-cancer drug which inhibits ATPase activity of topoisomerase II at micromolar concentrations.^[59,60] Similarly, as with VCE-003, various HU-331 analogues act as peroxisome proliferator activated receptors (PPAR) γ agonists and are predicted to have neuroprotective activities.^[61] HU-331 is also produced in mammals by hepatic microsomal enzymes where it forms adducts with glutathione.^[62] While it is unclear if these benzoquinone compounds could be an autoxidation artefact, a subset may represent *bona fide* natural products worth further investigation when considering the therapeutic potential of quinone cannabinoid derivatives.^[59–61]

In addition to the classical isoprenylated resorcinyl polyketide phytocannabinoids, other interesting PUFA-derived cannabinimimetic-like compounds were found as DAMs across female versus male floral samples. *N*-Acyl-ethanolamines are ubiquitous chemical signalling lipids which can potentiate responses of the mammalian endocannabinoid anandamide signalling pathway.^[63,64] Two such compounds, α -linolenoyl ethanolamide and palmitoyl ethanolamide, were found to be upregulated in male flowers (Table 3 and Fig. 5). While it is uncertain if the concentrations present would modify phytocannabinoid ligand activity, the presence of these compounds in male flowers is nonetheless intriguing.

Conclusion

This pilot study sought to both substantiate the methodological pipeline for tissue/organ comparative metabolome analyses by UHPLC-ESI-HRMS and to examine metabolic variation between unisexual flowers of the dioecious plant genus *Cannabis*. Our data indicate that this approach was successful in identifying several metabolites associated with sexual phenotype.

The chemical complexity of female flowers is evident from the PCA of floral tissues, with the metabolomes of the three female accessions showing a high level of dissimilarity

(Fig. 1b). A large proportion of this metabolic variation is not currently accounted for in the manufacture of crude herbal formulations, artisanal extracts, and magistral preparations intended for human consumption.^[34] While medicinal chemotypes of *Cannabis* are most commonly maintained through clonal propagation under controlled environment conditions,^[65,66] seed-grown industrial hemp sub-taxa are increasingly being used as feedstock for either nutraceutical or therapeutic-based products.^[67] Given the outcrossing and highly heterozygote nature of *Cannabis* plants in general, this could generate significant chemical variation which may have consequences for the quality, safety, and efficacy of *Cannabis* preparations.

Notwithstanding the targeted measurement of 14 major and minor cannabinoids, we identified several putative unknown phytocannabinoid-like metabolites upregulated in female flowers but were unable to unequivocally assign annotations to these compounds. The annotation of metabolites was limited by the availability of reference compounds to compare observed MS¹ and MS² information for correct annotation, thus highlighting the need to establish a comprehensive reference library or database for *Cannabis* metabolites. Development of phytocannabinoid-specific accurate-mass MSⁿ fragmentation spectral libraries coupled with nuclear magnetic resonance analysis will improve the confidence of compound structure annotation and mitigate challenges associated with the discrimination of multiple cannabinoid species and their constituent isomers and stereoisomers within complex botanical matrices.^[6,68] Moreover, the completion of a well annotated gene pool-representative *Cannabis* metabolome compiled from various plant tissues is predicted to improve small molecule and pathway analysis, thereby allowing comprehensive evaluation of metabolic variation underlying trait diversity. These resources will ultimately pave the way for contemporary multi-omics-based breeding strategies capable of facilitating metabolic engineering and genetic improvement of *Cannabis* for a variety of end-uses, therapeutic or industrial.

Experimental

Genetic Materials and Cultivation of Industrial Hemp *Cannabis* Germplasm

All research activities, including the procurement and cultivation of industrial hemp *Cannabis* germplasm, were carried out in accordance with Part IVA of the Drugs, Poisons and Controlled Substances Act 1981, and under an authorisation issued by Agriculture Victoria, Department of Jobs, Precincts and Regions (DJPR), Victorian State Government, Australia.

Seed from six industrial hemp *Cannabis sativa* L. accessions (varieties) were kindly provided *gratis* under permit from University and commercial sources within Australia (Table 1). Seeds were individually sown into seedling trays containing soil media at a depth of 1.5 cm and sprayed with reverse osmosis (RO) water daily until germination. Seedlings were transplanted into 400 mL pots and then transferred into 8 L pots at the emergence of the first (at ~1 week after sowing) and fourth leaflet pair (at ~3 weeks after sowing), respectively. Soil media consisted of one-part perlite, one-part peat moss, and one-part vermiculite as well as dolomite at a concentration of 1.1 g L⁻¹. Plants were grown in a controlled environment room (CER) at 24°C with 55 % humidity. The photoperiod was initially set to a long-day cycle (18/6 h light/dark) to promote vegetative growth and plants were watered daily using RO water supplemented

with CANNA Aqua Vega nutrient solution (40 mL CANNA Aqua Vega 1 and 40 mL CANNA Aqua Vega 2 in 10 L RO water). After 14 days, a shorter-day photoperiod (12/12 h light/dark) was maintained to initiate flowering and from this period, plants were watered daily with CANNA Classic Flores nutrient solution (40 mL Canna Flores A and 40 mL Canna Flores B in 10 L RO water) until harvest. Plants were harvested at maturation when ~95 % of the stigma on female flowers were browned and shrivelled or when ~95 % of male flowers had opened and expelled pollen. For each accession, floral tissue was taken from the apical (top 30 cm) and basal (bottom 30 cm) inflorescence and 1st, 2nd, and 3rd order foliage leaves were manually removed from floral samples before drying. All plants were destroyed during sample collection and were not used for further propagation.

Reagents and Standards

LC-MS grade methanol (Lichrosolv) used for extraction was purchased from Merck (Sigma Aldrich, NSW, Australia). Water with 0.1 % (v/v) formic acid (Optima LC-MS grade, mobile phase A), acetonitrile with 0.1 % (v/v) formic acid (Optima LCMS grade, mobile phase B), and Pierce FlexMix calibration solution were purchased from Thermo Fisher Scientific Inc. (Scoresby, Vic., Australia).

Cannabinoid certified reference standards in 1.0 mg mL⁻¹ solution in ampoules were purchased from Novachem Pty Ltd (Heidelberg West, Vic., Australia) as distributor for Cerilliant Corporation (Round Rock, Texas, USA). Cannabidiol (CBD), Δ^9 -tetrahydrocannabinol (Δ^9 -THC), cannabinol (CBN), cannabichromene (CBC), cannabigerol (CBG), cannabidivarin (CBDV), and tetrahydrocannabivarin (THCV) were in methanol. Cannabidiolic acid (CBDA), Δ^9 -tetrahydrocannabinolic acid A (Δ^9 -THCAA), cannabinolic acid (CBNA), cannabichromenic acid (CBCA), cannabigerolic acid (CBGA), cannabidivarinic acid (CBDVA), and tetrahydrocannabivarinic acid (THCVA) were in acetonitrile. A mixed standard of CBD, Δ^9 -THC, CBN, CBC, CBDV, and THCV (Standard Set 1) was prepared at 200 μ g mL⁻¹ in methanol and diluted to prepare the working standards at 0.1, 0.5, 1, 5, 10, 25, 50, and 100 μ g mL⁻¹. A mixed standard of CBDA, Δ^9 -THCAA, CBNA, CBCA, CBDVA, and THCVA (Standard Set 2) was prepared at 150 μ g mL⁻¹ in acetonitrile and diluted to prepare the working standards at 0.1, 0.5, 1, 5, 25, 50, 75, and 100 μ g mL⁻¹. CBG (Standard Set 3) and CBGA (Standard Set 4) were prepared separately at 200 μ g mL⁻¹ in acetonitrile and methanol, respectively, and diluted to 0.1, 0.5, 1, 5, 25, 50, 75, and 100 μ g mL⁻¹. All standard solutions were stored at -80°C.

Sample Preparation

Male and female floral samples were dried in a Thermo Scientific Heratherm gravity convection oven at 40°C for 96 h. Seeds and stalks were manually separated using a coarse sieve and discarded. For male inflorescences, panicles comprising of staminate flowers and \geq 4th order reduced leaves were retained, while for female inflorescences, phytomere tissues comprising of pistillate flowers, perigonal bracts, bracts, and \geq 4th order reduced leaves remained. Inflorescence material was homogenised in a Geno/Grinder 2010 (Spex SamplePrep, Metuchen, NJ, USA) at 1500 rpm for 2 \times 30 s intervals in 15 mL short polycarbonate vials with stainless steel grinding balls. Fifty milligrams (50 mg) of finely ground floral tissue was weighed into an Eppendorf Safe-Lock microcentrifuge tube and

extracted in 5 mL of LCMS-grade methanol with vortex mixing (1 min) and sonication at room temperature for 20 min. The mixture was allowed to sit for a few minutes and then filtered through a 0.45 μm polytetrafluoroethylene (PTFE) syringe filter. Each sample extract was diluted 10 \times with methanol. Aliquots of the filtrate were transferred to 2 mL amber HPLC vials and stored at -80°C before analysis. Three extraction replicates were performed on each apical and basal floral tissue sample, totalling six extraction (technical) replicates per accession.

Ultra-High-Performance Liquid Chromatography–High-Resolution Mass Spectrometry (UHPLC–HRMS) Analysis

UHPLC–HRMS separation, detection, and analysis of diluted and undiluted extracts was carried out on a Thermo Fisher Vanquish Flex UHPLC system with solvent degasser, quaternary pump, temperature-controlled sampler/auto injector (maintained at 5°C), temperature-regulated column compartment maintained at 30°C , and photodiode array detector (DAD) coupled to an Orbitrap ID-X Tribrid high resolution mass spectrometer (Thermo Fisher Scientific Inc., MA, USA). Separation was carried out on a Phenomenex Kinetex C_{18} column, 1.7 μm , 150 mm \times 2.1 mm (Phenomenex Australia Pty Ltd, NSW, Australia). Mobile phases used were water with 0.1 % (v/v) formic acid (mobile phase A) and acetonitrile with 0.1 % (v/v) formic acid (mobile phase B) with 0.3 mL min^{-1} flow rate using the following gradient program: 10 % B, 0–2 min; 10 to 40 % B, 2–3 min; 40 % B, 3–5 min; 40 to 80 % B, 5–6 min; 80 % B, 6–9 min; 80 to 90 % B, 9–11 min; 90 to 100 % B, 11–12 min; 100 % B, 12–15 min; 100 to 10 % B, 15–16 min; and 10 % B from 16–20 min. Injection volume was 3 μL .

MS analysis was carried out using an electrospray ionisation (ESI) interface in the positive ion mode. Resolution was 120 000 in full scan mode and 15 000 in data dependent MS^2 with HCD activation, with both MS and MS^2 using the orbitrap as the mass analyser and a mass range of m/z 100 to 1000. Sheath and auxiliary gases were nitrogen at 50 and 10 arbitrary units (a.u.), respectively. ESI spray voltage was 3.5 kV, and the capillary and vaporiser temperatures were 325 and 350°C , respectively. Prior to data acquisition, the MS was calibrated with Pierce FlexMix calibration solution and the internal mass calibrant fluoranthene (Easy-IC) was activated during data acquisition for real-time mass calibration. Software for data acquisition was *Xcalibur 4.4*.

MS Data Processing and Statistical Analysis

Full MS data were processed using *Trace Finder 4.1* (Thermo Fisher Scientific Inc., MA, USA) for quantitative analysis. Peak identity was determined by comparison of retention time with reference standards and integration of extracted ion peaks. The concentration of each analyte was determined by interpolation from standard calibration curves generated in MS Excel and results were expressed as average concentration \pm standard deviation (s.d.).

The high-resolution accurate mass (HRAM) data were further processed using Thermo Scientific *Compound Discoverer 3.1* software. The following parameters were used for aligning retention times: alignment model = adaptive curve; maximum shift [min] = 2; mass tolerance [ppm] = 5. The following parameters were used for compound detection: mass tolerance [ppm] = 5; intensity tolerance [%] = 30; S/N threshold = 3; min peak intensity = 50000; Ions = $[\text{M} + \text{H}]^+1$, $[\text{M} + \text{H} - \text{H}_2\text{O}]^+1$; Base Ions = $[\text{M} + \text{H}]^+1$, $[\text{M} - \text{H}]^-1$; min element counts = C H; max. element counts = $\text{C}_{100} \text{H}_{300} \text{Br}_5 \text{Cl}_{10} \text{K}_5 \text{N}_{20} \text{Na}_5 \text{O}_{50} \text{P}_{10} \text{S}_{10}$. To eliminate drift and correct for batch effects, peak area was

normalised linearly using the area under the peak of the quality control (QC) sample. QC samples were developed from pooled male and female floral tissue samples and these were measured every nine injections. QC-corrected chromatographic peak area data was used for statistical analysis. For principle component analysis (PCA), PC1 and PC2 data points were centred and scaled. Euclidean distance was the distance measure used for hierarchical cluster analysis (HCA). To detect differential metabolites between male and female floral tissues, volcano plot analysis using Student's *t*-test was performed, with adjusted *P*-values calculated using the Benjamini–Hochberg correction for the false-discovery rate.

Compound Annotation

Small-molecule identification was performed using Thermo Scientific *Compound Discoverer 3.1* software, with annotation of putative compounds achieved using consensus evaluation from calculated elemental composition and searches using HRAM MS^n spectral library mzCloud and compound database ChemSpider along with fragment ion searching (FISH) to predict *in silico* fragmentation and ranking (mzLogic) algorithmic tools. For mzCloud searches, the following parameters were used: compound classes = all; precursor mass tolerance [ppm] = 10; FT fragment mass tolerance [ppm] = 10; IT fragment mass tolerance [Da] = 0.4; Library = auto processed, reference; post processing = recalibrated; max # results = 10; annotate matching fragments = true. DDA search parameters were as follows: identity search = cosine; match activation type = true; match activation energy = match with tolerance; activation energy tolerance = 20; apply intensity threshold = true; similarity search = confidence forward; match factor threshold = 60. ChemSpider searches included the following databases: Cambridge Structural Database; Carotenoids Database; DrugBank; KEGG; LipidMAPS; NIST Chemistry WebBook; Phenol-Explorer; PlantCyc; PubMed. Searches were conducted by Formula and Mass using the following parameters: mass tolerance [ppm] = 5 ppm; max. # of results per compound = 100; max. # of predicted compositions searched per compound = 3. mzLogic was applied with the following parameters: FT fragment mass tolerance [ppm] = 10; IT fragment mass tolerance [Da] = 0.4; max. # compounds = 0; max. # mzCloud similarity results to consider per compound = 10; match factor threshold = 30. FISH scoring settings used were high accuracy mass tolerance = 5 ppm; low accuracy mass tolerance = 20 ppm; S/N threshold = 3; max depth = 5.

Metabolic Pathways Enrichment Analysis

To interpret the biological significance associated with metabolite changes between female vs male floral tissues, Kyoto Encyclopedia of Genes and Genomes (KEGG, website: <https://www.genome.jp/kegg/pathway.html>) pathway over-representation (enrichment) analysis was performed on putative differential metabolites using the Metabolites Biological Role (MBRole) server.^[69] KEGG compound IDs which served as input for enrichment analysis were retrieved from *Compound Discoverer* software (v 3.11.12). At the time of analysis, neither a metabolome nor a reference set of compounds for *Cannabis sativa* was available and so the background set was based on all compounds in the database associated with KEGG pathway annotations. Enrichment *p*-values were adjusted for multiple testing using the Benjamini–Hochberg correction for the false-discovery rate.^[70]

Supplementary Material

The list of putative compounds identified from male and female flowers, KEGG enrichment of differentially regulated metabolic pathways, and principal component analysis loadings and variances plots of metabolite abundances, as well as MS² spectral data of HU-331 and unknown compounds are available on the Journal's website. Table S1: List of 2599 putative compounds identified from male and female flowers; Table S2: KEGG enrichment of differentially regulated metabolic pathways in female v. male floral tissues; Table S3: Consensus annotation of 41 DAMs; Fig. S1: Principal component analysis loadings and variances plots of metabolite abundances from male and female floral tissue samples; Appendix S1: MS² spectral data of 11 compounds that were initially annotated as HU-331; and Appendix S2: MS² spectral data of HU-331.

Conflicts of Interest

The authors declare no conflicts of interest.

Declaration of Funding

MSD, AB, and MTW acknowledge the support of the Australian Research Council (ARC) Linkage Program grant (LP160101317). AB, MSD, and MAD acknowledge the support of the ARC Research Hub for Medicinal Agriculture (IH180100006). Cann Group Limited are a partner organisation of the ARC linkage program grant LP160101317 and the ARC Research Hub for Medicinal Agriculture (IH180100006). The authors also acknowledge generous resource allocations from an Ian Potter Foundation grant (#31110299) and the ARC LIEF scheme grant (LE200100117) towards the purchase of the mass spectrometers. AB and MSD were supported by La Trobe University through the La Trobe Institute for Agriculture and Food (LIAF).

References

- [1] J. M. McPartland, W. Hegman, T. Long, *Veg. Hist. Archaeobot.* **2019**, 28, 691. doi:10.1007/S00334-019-00731-8
- [2] E. Small, *Bot. Rev.* **2015**, 81, 306. doi:10.1007/S12229-015-9159-1
- [3] E. Small, A. Cronquist, *Taxon* **1976**, 25, 405. doi:10.2307/1220524
- [4] R. H. W. Bradshaw, P. Coxon, J. R. A. Greig, A. R. Hall, *New Phytol.* **1981**, 89, 503. doi:10.1111/J.1469-8137.1981.TB02331.X
- [5] I. J. Flores-Sanchez, R. Verpoorte, *Phytochem. Rev.* **2008**, 7, 615. doi:10.1007/S11101-008-9094-4
- [6] L. O. Hanuš, S. M. Meyer, E. Muñoz, O. Tagliatalata-Scafati, G. Appendino, *Nat. Prod. Rep.* **2016**, 33, 1357. doi:10.1039/C6NP00074F
- [7] E. D. French, *Neurosci. Lett.* **1997**, 226, 159. doi:10.1016/S0304-3940(97)00278-4
- [8] O. Devinsky, J. H. Cross, L. Laux, E. Marsh, I. Miller, R. Nababout, *et al.*, *N. Engl. J. Med.* **2017**, 376, 2011. doi:10.2337/DC16-0650
- [9] M. Heblinski, M. Santiago, C. Fletcher, J. Stuart, M. Connor, I. S. McGregor, *et al.*, *Cannabis Cannabinoid Res.* **2020**, 5, 305. doi:10.1089/CAN.2019.0099
- [10] C. Staginuss, S. Zörntlein, E. de Meijer, *J. Forensic Sci.* **2014**, 59, 919. doi:10.1111/1556-4029.12448
- [11] M. T. Welling, L. Liu, C. A. Raymond, T. Kretschmar, O. Ansari, G. J. King, *Sci. Rep.* **2019**, 9, 11421. doi:10.1038/S41598-019-47812-2
- [12] S. J. Livingston, T. D. Quilichini, J. K. Booth, D. C. Wong, K. H. Rensing, J. Laflamme-Yonkman, *et al.*, *Plant J.* **2020**, 101, 37. doi:10.1111/TPJ.14516
- [13] N. Happyana, S. Agnolet, R. Muntendam, A. Van Dam, B. Schneider, O. Kayser, *Phytochemistry* **2013**, 87, 51. doi:10.1016/J.PHYTOCHEM.2012.11.001
- [14] B. Spitzer-Rimon, S. Duchin, N. Bernstein, R. Kamenetsky, *Front. Plant Sci.* **2019**, 10, 350. doi:10.3389/FPLS.2019.00350
- [15] V. C. Moliterni, L. Cattivelli, P. Ranalli, G. Mandolino, *Euphytica* **2004**, 140, 95. doi:10.1007/S10681-004-4758-7
- [16] Z. K. Punja, J. E. Holmes, *Front. Plant Sci.* **2020**, 11, 718. doi:10.3389/FPLS.2020.00718
- [17] J. Petit, E. M. Salentijn, M.-J. Paulo, C. Thouminot, B. J. van Dinter, G. Magagnini, *et al.*, *Front. Plant Sci.* **2020**, 11, 102. doi:10.3389/FPLS.2020.00102
- [18] M. G. Divashuk, O. S. Alexandrov, O. V. Razumova, I. V. Kirov, G. I. Karlov, *PLoS One* **2014**, 9, e85118. doi:10.1371/JOURNAL.PONE.0085118
- [19] J. D. Lubell, M. H. Brand, *Horttechnology* **2018**, 28, 743. doi:10.21273/HORTTECH04188-18
- [20] H. M. Ram, V. S. Jaiswal, *Planta* **1972**, 105, 263. doi:10.1007/BF00385397
- [21] N. Sriram, H. M. Ram, *Curr. Sci.* **1984**, 53, 735.
- [22] G. Mandolino, A. Carboni, *Euphytica* **2004**, 140, 107. doi:10.1007/S10681-004-4759-6
- [23] E. Small, S. G. Naraine, *Genet. Resour. Crop Evol.* **2016**, 63, 339. doi:10.1007/S10722-015-0253-3
- [24] A.-M. Faux, X. Draye, R. Lambert, R. d'Andrimont, P. Raulier, P. Bertin, *Eur. J. Agron.* **2013**, 47, 11. doi:10.1016/J.EJA.2013.01.006
- [25] D. U. Nagy, K. Cianfaglione, F. Maggi, S. Sut, S. Dall'Acqua, *Chem. Biodivers.* **2019**, 16, e1800562. doi:10.1002/CBDV.201800562
- [26] A. Ohlsson, C. Abou-Chaar, S. Agurell, I. Nilsson, K. Olofsson, F. Sandberg, *Bull. Narc.* **1971**, 23, 29.
- [27] R. Latta, B. Eaton, *Econ. Bot.* **1975**, 29, 153. doi:10.1007/BF02863315
- [28] H. Kushima, Y. Shoyama, I. Nishioka, *Chem. Pharm. Bull.* **1980**, 28, 594. doi:10.1248/CPB.28.594
- [29] A. Cerrato, G. Cannazza, A. L. Capriotti, C. Citti, G. La Barbera, A. Laganà, *et al.*, *Talanta* **2020**, 209, 120573. doi:10.1016/J.TALANTA.2019.120573
- [30] B. Hurgobin, M. Tamiru-Oli, M. T. Welling, M. S. Doblin, A. Bacic, J. Whelan, *et al.*, *New Phytol.* **2021**, 230, 73. doi:10.1111/NPH.17140
- [31] G. Nyamundanda, I. C. Gormley, Y. Fan, W. M. Gallagher, L. Brennan, *BMC Bioinformatics* **2013**, 14, 338. doi:10.1186/1471-2105-14-338
- [32] D. Dudzik, C. Barbas-Bernardos, A. Garcia, C. Barbas, *J. Pharm. Biomed. Anal.* **2018**, 147, 149. doi:10.1016/J.JPBA.2017.07.044
- [33] B. Worley, R. Powers, *Curr. Metabolomics* **2013**, 1, 92.
- [34] C. Citti, U. M. Battisti, D. Braghiroli, G. Ciccarella, M. Schmid, M. A. Vandelli, *et al.*, *Phytochem. Anal.* **2018**, 29, 144. doi:10.1002/PCA.2722
- [35] L. W. Sumner, A. Amberg, D. Barrett, M. H. Beale, R. Beger, C. A. Daykin, *et al.*, *Metabolomics* **2007**, 3, 211. doi:10.1007/S11306-007-0082-2
- [36] P. Dayanandan, P. B. Kaufman, *Am. J. Bot.* **1976**, 63, 578. doi:10.1002/J.1537-2197.1976.TB11846.X
- [37] E. P. M. de Meijer, K. M. Hammond, *Euphytica* **2016**, 210, 291. doi:10.1007/S10681-016-1721-3
- [38] B. Ylstra, A. Touraev, R. M. B. Moreno, E. Stöger, A. J. Van Tunen, O. Vicente, *et al.*, *Plant Physiol.* **1992**, 100, 902. doi:10.1104/PP.100.2.902
- [39] L. Taylor, R. Jorgensen, *J. Hered.* **1992**, 83, 11. doi:10.1093/OXFORDJOURNALS.JHERED.A111149
- [40] E. G. Schijlen, C. R. de Vos, S. Martens, H. H. Jonker, F. M. Rosin, J. W. Molthoff, *et al.*, *Plant Physiol.* **2007**, 144, 1520. doi:10.1104/PP.107.100305
- [41] X. Ding, X. Wang, Q. Li, L. Yu, Q. Song, J. Gai, *et al.*, *Int. J. Mol. Sci.* **2019**, 20, 2869. doi:10.3390/IJMS20122869
- [42] A. P. Brown, J. T. Kroon, D. Swarbreck, M. Febrer, T. R. Larson, I. A. Graham, *et al.*, *PLoS One* **2012**, 7, e30100. doi:10.1371/JOURNAL.PONE.0030100
- [43] N. E. Rothnie, M. V. Palmer, D. G. Burke, J. P. Sang, E. P. Hilliard, P. A. Salisbury, *et al.*, *Phytochemistry* **1987**, 26, 1895. doi:10.1016/S0031-9422(00)81723-9
- [44] F. Opute, *Phytochemistry* **1975**, 14, 1023. doi:10.1016/0031-9422(75)85180-6

- [45] A. Dave, I. A. Graham, *Front. Plant Sci.* **2012**, *3*, 42. doi:10.3389/FPLS.2012.00042
- [46] N. Taki, Y. Sasaki-Sekimoto, T. Obayashi, A. Kikuta, K. Kobayashi, T. Aina, *et al.*, *Plant Physiol.* **2005**, *139*, 1268. doi:10.1104/PP.105.067058
- [47] A. Moreno-Rodríguez, R. Santos-Castro, J. Vázquez-Medrano, R. E. Quintanar-Zúñiga, F. A. García-García, L. B. Hernández-Portilla, *et al.*, *Nat. Prod. Res.* **2020**, *34*, 1942. doi:10.1080/14786419.2019.1566721
- [48] H. Enomoto, T. Senu, K. Sato, F. Sato, T. Paxton, E. Yumoto, *et al.*, *Sci. Rep.* **2017**, *7*, 42977. doi:10.1038/SREP42977
- [49] S. Goetz, A. Hellwege, I. Stenzel, C. Kutter, V. Hauptmann, S. Forner, *et al.*, *Plant Physiol.* **2012**, *158*, 1715. doi:10.1104/PP.111.192658
- [50] K. Wang, Q. Guo, J. E. Froehlich, H. L. Hersh, A. Zienkiewicz, G. A. Howe, *et al.*, *Plant Cell* **2018**, *30*, 1006. doi:10.1105/TPC.18.00250
- [51] E. Galoch, *Acta Soc. Bot. Pol.* **1978**, *47*, 153. doi:10.5586/ASBP.1978.013
- [52] M. Hofinger, *Arch. Int. Physiol. Biochim.* **1969**, *77*, 225. doi:10.3109/13813456909109702
- [53] F. Salari, H. Mansori, *Journal of Plant Process and Function* **2013**, *1*, 51.
- [54] H. Mansouri, Z. Asrar, J. Szopa, *Plant Growth Regul.* **2009**, *58*, 269. doi:10.1007/S10725-009-9375-Y
- [55] A. M. Adal, K. Doshi, L. Holbrook, S. S. Mahmoud, *Planta* **2021**, *253*, 17. doi:10.1007/S00425-020-03522-Y
- [56] R. Mechoulam, Z. Ben-Zvi, Y. Gaoni, *Tetrahedron* **1968**, *24*, 5615. doi:10.1016/0040-4020(68)88159-1
- [57] N. M. Kogan, R. Rabinowitz, P. Levi, D. Gibson, P. Sandor, M. Schlesinger, *et al.*, *J. Med. Chem.* **2004**, *47*, 3800. doi:10.1021/JM040042O
- [58] J. Díaz-Alonso, J. Paraíso-Luna, C. Navarrete, C. Del Río, I. Cantarero, B. Palomares, *et al.*, *Sci. Rep.* **2016**, *6*, 29789. doi:10.1038/SREP29789
- [59] K. M. Regal, S. L. Mercer, J. E. Deweese, *Chem. Res. Toxicol.* **2014**, *27*, 2044. doi:10.1021/TX500245M
- [60] J. T. Wilson, C. A. Fief, K. D. Jackson, S. L. Mercer, J. E. Deweese, *Chem. Res. Toxicol.* **2018**, *31*, 137. doi:10.1021/ACS.CHEMRES TOX.7B00302
- [61] R. Mechoulam, L. Hanuš, *Chem. Phys. Lipids* **2002**, *121*, 35. doi:10.1016/S0009-3084(02)00144-5
- [62] L. M. Bornheim, M. P. Grillo, *Chem. Res. Toxicol.* **1998**, *11*, 1209. doi:10.1021/TX9800598
- [63] E. Palazzo, L. Luongo, F. Guida, V. de Novellis, S. Boccella, C. Cristiano, *et al.*, *Neuropsychiatry* **2019**, *9*, 2035.
- [64] S. Petrosino, V. Di Marzo, *Br. J. Pharmacol.* **2017**, *174*, 1349. doi:10.1111/BPH.13580
- [65] O. Aizpurua-Olaizola, U. Soydaner, E. Öztürk, D. Schibano, Y. Simsir, P. Navarro, *et al.*, *J. Nat. Prod.* **2016**, *79*, 324. doi:10.1021/ACS.JNATPROD.5B00949
- [66] B. De Backer, K. Maebe, A. G. Verstraete, C. Charlier, *J. Forensic Sci.* **2012**, *57*, 918. doi:10.1111/J.1556-4029.2012.02068.X
- [67] S. Chandra, H. Lata, M. A. ElSohly, L. A. Walker, D. Potter, *Epilepsy Behav.* **2017**, *70*, 302. doi:10.1016/J.YEBEH.2016.11.029
- [68] C. Citti, F. Russo, S. Sgrò, A. Gallo, A. Zanotto, F. Forni, *et al.*, *Anal. Bioanal. Chem.* **2020**, *412*, 4009. doi:10.1007/S00216-020-02554-3
- [69] J. López-Ibáñez, F. Pazos, M. Chagoyen, *Nucleic Acids Res.* **2016**, *44*, W201. doi:10.1093/NAR/GKW253
- [70] Y. Benjamini, Y. Hochberg, *J. R. Stat. Soc. B* **1995**, *57*, 289. doi:10.1111/J.2517-6161.1995.TB02031.X

Handling Editor: Charlotte Williams